



HAL
open science

Dual-band, dual-linearly polarized transmitarrays for SATCOM applications at Ka-band

Reda Madi, Ronan Sauleau, Antonio Clemente

► **To cite this version:**

Reda Madi, Ronan Sauleau, Antonio Clemente. Dual-band, dual-linearly polarized transmitarrays for SATCOM applications at Ka-band. EUcap 2022 - The 16th European Conference on Antennas and Propagation, Mar 2022, Madrid, Spain. cea-03637073

HAL Id: cea-03637073

<https://cea.hal.science/cea-03637073>

Submitted on 11 Apr 2022

HAL is a multi-disciplinary open access archive for the deposit and dissemination of scientific research documents, whether they are published or not. The documents may come from teaching and research institutions in France or abroad, or from public or private research centers.

L'archive ouverte pluridisciplinaire **HAL**, est destinée au dépôt et à la diffusion de documents scientifiques de niveau recherche, publiés ou non, émanant des établissements d'enseignement et de recherche français ou étrangers, des laboratoires publics ou privés.

Dual-Band, Dual-Linearly Polarized Transmitarrays for SATCOM Applications at Ka-Band

Reda Madi[#], Antonio Clemente[#], Ronan Sauleau^{*}

[#]Univ. Grenoble-Alpes, CEA, Leti, F-38000, Grenoble, France

^{*}Univ. Rennes, CNRS, IETR, UMR 6164, F-35000 Rennes, France

antonio.clemente@cea.fr, ronan.sauleau@univ-rennes1.fr

Abstract—We propose here a 40×40-element shared-aperture dual-band dual linearly-polarized transmitarray with 1-bit phase resolution and fixed beam at Ka-band. The design is based on a stacked approach where the unit-cell size is compact and is equal to only $0.48\times\lambda_0$ and $0.32\times\lambda_0$ at 29 GHz and 19 GHz, respectively. The beam-scanning performances of this array are compared to those of an array with the same number of elements and same illumination but comprising unit-cells based on the interleaving approach (lattice size of $0.72\times\lambda_0$ and $0.47\times\lambda_0$, respectively). The shared-aperture unit-cells include four printed U-slotted patch antennas and a connecting metallized via; the desired 180° phase shift is obtained by rotating one of the patches around its corresponding via. Our simulation results demonstrate that the transmitarray based on the stacked approach exhibits excellent beam scanning performance up to $\pm 70^\circ$ on the two bands. A prototype pointing at broadside has been optimized and fabricated to validate the numerical simulations.

Index Terms—Transmitarray antenna, SATCOM, dual-band, dual-linear polarization.

I. INTRODUCTION

The development of broadband satellite communications (SATCOM) and SATCOM-on-the-move (SOTM) at Ka-band requires innovative antenna architectures with electronically beam-forming capabilities in full duplex (uplink and downlink) and dual-polarization.

In this context, phased arrays [1],[2] are an attractive solution compared to more standard mechanically-steerable antennas; but they lead to relatively complex, expensive, and power consuming systems.

As an alternative, transmitarrays represent a rather mature and cost-effective technology achieving radiation efficiency better than phased arrays, thanks to the spatial feeding mechanism, and, at the same time, fine two-dimensional (2D) beam steering capability. A transmitarray antenna is typically composed of a feed and, at a relatively short distance, a planar array of elements, which introduce proper local phase shifts on the incident wave, in order to collimate the radiated beam in a predefined direction and/or generate a specific radiation pattern [3]. Electronically beam-scanning can be also implemented by integrating varactors [4], MEMS [5], or p-i-n diodes [6],[7] in the unit-cells.

Several dual-band dual-polarized transmitarrays with fixed-beam and shared Tx/Rx aperture have been

demonstrated in the open literature at Ku and Ka-bands [8]-[14]. To the best of our knowledge, the lattice size of all these prototypes is larger than half a wavelength. This constitutes a key limitation for beam scanning applications due to the appearance of grating lobes in the visible range.

To circumvent this limitation, we introduce here a new dual-band dual-linearly polarized unit-cell for transmitarray at Ka-band. This unit-cell is based on a stacked approach where the Tx unit-cell and Rx unit-cell are placed one on top of the other. The overall lattice size is very compact, with a size of $0.48\times\lambda_0$ and $0.32\times\lambda_0$ at the uplink (27.5 – 31 GHz) and downlink (17 – 21 GHz) bands, respectively. This type of unit-cell has been developed for a future implementation of an electronically-scanned dual-band dual-polarized transmitarray.

We also compare here the proposed unit-cell with another unit-cell design based on the interleaving technique. Numerical simulations using our in-house CAD tool have been performed to study the beam-steering performance of both transmitarray configurations (namely, stacked vs. interleaved); the selected test case is a 1600-element square transmitarray. Finally, a dual-band dual-linearly polarized transmitarray based on the proposed stacked unit-cells has been optimized, fabricated, and characterized in anechoic chamber to validate the proposed design methodology.

II. DUAL-BAND DUAL-LINEARLY POLARIZED UNIT-CELL DESIGNS

The two proposed unit-cell designs are represented in Fig. 1. In the first one (UC#1), the dual-band operation relies on interleaving two orthogonally polarized patches operating in either downlink or uplink band. For the second design (UC#2), the dual-band functionality is achieved by stacking orthogonally-polarized radiating elements. For this study, both architectures use four U-slotted patch antennas (i.e. two patches printed on the Rx layers and two on the Tx layers), operating at 19 GHz for the lower frequency band (downlink) and at 29 GHz for the upper frequency band (uplink). The U-slotted architecture is selected to achieve a wideband behavior in both frequency bands. The same dielectric materials are used for both configurations, i.e. Roger RT/Duroid 6002 substrates ($\epsilon_r = 2.94$, $\tan\delta = 0.0012$) and a thin bounding film, Arlon CuClad 6700 ($\epsilon_r = 2.35$, and $\tan\delta = 0.0025$). The use of a metallized via to connect

the Rx and Tx patch antennas allows us to achieve a 1-bit phase resolution over a broadband. The phase-shift introduced in each frequency band is essentially independent and is achieved by rotating by 180° the Tx patches (or equivalently the Rx patches) around the via. These unit-cell architectures are described more in details in Sections II.A and II.B, respectively.

A. Unit-Cell based on the Interleaving Approach

The first unit-cell (UC#1) architecture relies on the interleaving technique. This method consists in arranging two orthogonally-polarized elements printed on the same layer (one for the downlink, and one for the uplink). The dielectric stack-up is composed of three metallic layers (Rx patches, ground plane, and Tx patches) printed on two 0.508-mm thick substrates, as represented in Fig. 1(a). A bonding film is used to glue both substrates. Since the two elements are orthogonally polarized and weakly coupled, they can be designed almost separately, thus simplifying considerably the design procedure and maintaining the dual-band operation. The lattice periodicity is equal to $0.72 \times \lambda_0$ and $0.47 \times \lambda_0$ at the uplink (27.5 – 31 GHz) and downlink (17 – 21 GHz) bands, respectively.

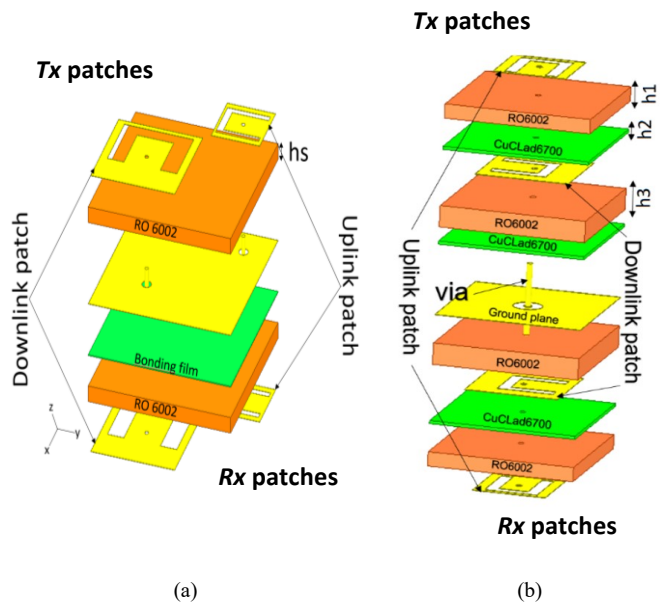


Fig. 1. 3D view of the proposed unit-cells based on interleaving (a) and stacked (b) methods.

B. Unit-Cell based on the stacked Approach

For this unit-cell (UC#2), the orthogonally-polarized elements are stacked on two different layers. This configuration leads to a much more compact lattice size. This technique has already been introduced in our preliminary paper [15]. The unit-cell stack-up is made of five metal layers (Rx patch for the uplink, Rx patch for the downlink, ground plane, Tx patch for the downlink, and Tx patch for the uplink) printed on four different dielectric substrates.

Three bonding films are used to glue the dielectric layers. The inner substrates have thickness of 0.762 mm, while the thickness of the outer ones is 0.508 mm. The radiating elements operating in the uplink are printed on the top and bottom metal layers, while the downlink patches are printed on two of the three inner layers. The unit-cell stack-up is represented in Fig. 1(b). The periodicity is equal to $0.48 \times \lambda_0$ and $0.32 \times \lambda_0$ at the uplink and downlink bands, respectively. As the design of such a unit-cell is more challenging than UC#1, extensive full-wave simulations have been carried out. More detail will be provided during the conference.

C. Simulation Results

The proposed unit-cells have been simulated using the full-wave electromagnetic software Ansys HFSS (v.20.1) with periodic boundary conditions and Floquet ports. Dielectric and ohmic losses are taken into account in the simulations. The transmission phase of the simulated scattering parameters computed under normal incidence is depicted in Fig. 2. Here, the unit-cell using the interleaving method is denoted with UC#1, and the unit-cell using the superposition method is labelled UC#2.

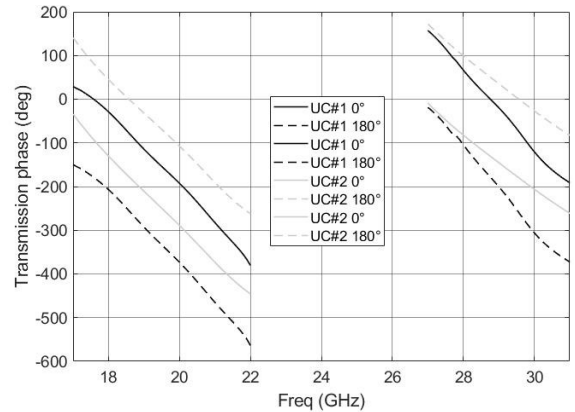


Fig. 2. Computed transmission phase of UC#1 and UC#2.

As shown in Fig. 2, a 180° relative phase shift is achieved over the entire bandwidth of interest with a maximum phase error of 4.4° and 9.1° for UC#1 and 4.6° and 1.6° for UC#2 in the lower and higher frequency bands, respectively. The main results are provided in Table I.

III. 40×40 ELEMENT TRANSMITARRAY: NUMERICAL ANALYSIS AND EXPERIMENTAL RESULTS

The performance of two 40×40 element transmitarrays (TA#1 and TA#2) based UC#1 and UC#2 are compared in Section III.A to evidence their main characteristics for beam scanning applications. Moreover, the performance of UC#2 are validated through the experimental characterization of a 1600-element transmitarray based on this unit-cell and pointing at broadside (Section III.B).

A. Numerical Analysis

The radiation characteristics of TA#1 and TA#2 are computed using our *in-house* CAD simulation tool (mostly based on array theory). A 10-dBi standard feed horn is used to illuminate these transmitarrays.

TABLE I. SIMULATED PERFORMANCE OF UNIT-CELL #1 AND UNIT-CELL #2 (DL: DOWNLINK; UL: UPLINK)

	UC#1		UC#2	
	DL	UL	DL	UL
Min IL (dB)	0.20	0.32	0.40	0.38
1-dB bandwidth (%)	13.2	7.10	17.4	10.7
3-dB bandwidth (%)	18.5	9.70	19.8	12.0
Period (λ)	0.47	0.72	0.33	0.48
Max Phase error ($^\circ$)	4.40	9.10	4.60	1.60

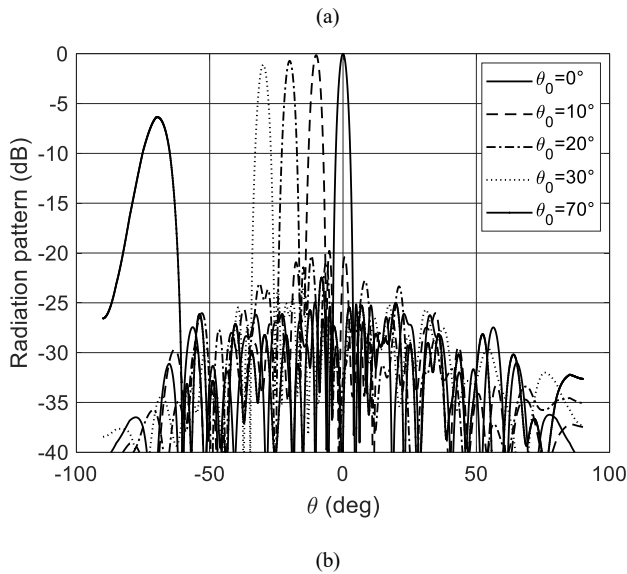
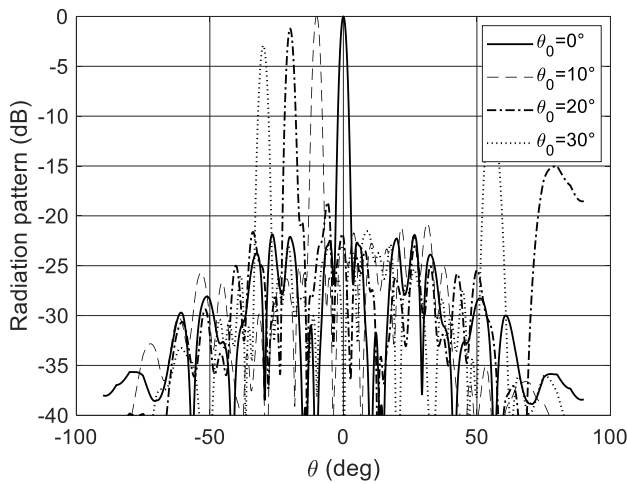
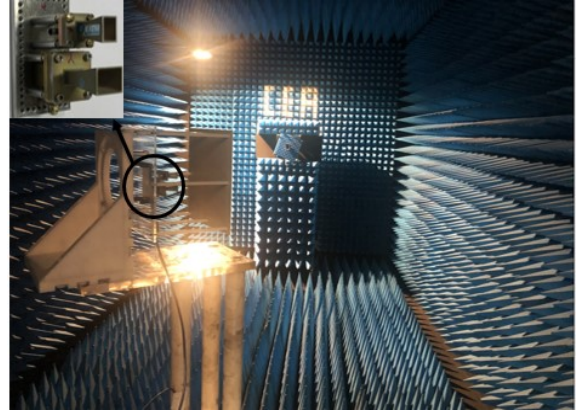


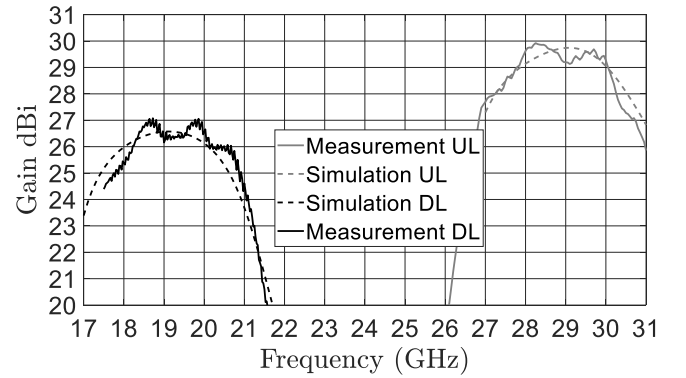
Fig. 3. Simulated radiation patterns for (a) TA#1 and (b) TA#2 for several main beam directions in the plane $\phi = 0^\circ$ at 29 GHz.

The performance in radiation is compared only at the higher frequency band, since the beam degradation due to the lattice size is more relevant in this frequency range.

The radiation patterns computed for several main beam directions in the cut-plane $\phi = 0^\circ$ are plotted in Fig. 3 at 29 GHz for both transmitarrays. For TA#1, grating lobes are clearly visible for beam pointing directions beyond 20° (Fig. 3(a)), with a gain drop of about 3 dB at 30° , while the maximum gain drop is only 1.5 dB for TA#2 in the same direction (Fig. 3(b)). Moreover, in this case, the beam quality is well preserved up to 70° .



(a)



(b)

Fig. 4. Measured 40×40-element TA#2: (a) photograph of the measured antenna and (b) frequency response in the uplink (UL) and downlink (DL) bands.

B. Prototyping and Experimental Characterization

A 40×40-element transmitarray has been designed, optimized, and fabricated to validate the proposed stacked unit-cell architecture (see Fig. 4(a)). Two standard 10-dBi gain horns have been used to illuminate the transmitarray. The selected focal distance is equal to 110 mm ($F/D = 0.56$). The uplink and downlink phase distributions are synthesized to collimate the beam at broadside. It is important to notice that an independent phase shift can be applied to steer the beam on two independent directions.

The transmitarray has been characterized in the CEA-Leti far-field anechoic chamber. The measured gain frequency response is plotted in Fig. 4(b). These data are in very satisfactory agreement with the numerical results. The measured peak gain is equal to 27.1 dBi at 19.8 GHz, corresponding to an aperture efficiency of 25.1%. In the uplink frequency band, a maximum gain of 29.9 dBi is achieved at 28.3 GHz, with an aperture efficiency of 20.1%.

IV. CONCLUSIONS

A new 1-bit dual-band dual-polarized unit-cell based on a stacked approach has been proposed here. Its architecture leads to a relatively compact design having a lattice period smaller than half a wavelength in the SATCOM down- and up-links at Ka band. A 40×40 transmitarray is optimized, fabricated and characterized to validate the design methodology.

ACKNOWLEDGMENT

This work was partly supported by the National Research Agency (ANR) through the project ANR-ASTRID ArtiKa under grant ANR-20-ASTR-0014-01.

REFERENCES

- [1] X. Luo, et al., "A scalable Ka-band 1024-element transmit dual-circularly-polarized planar phased array for SATCOM applications," *IEEE Access*, Sep. 2020.
- [2] K. K. Wei Low, A. Nafe, S. Zahir, T. Kanar and G. M. Rebeiz, "A scalable circularly-polarized 256-element Ka-band phased-array SATCOM transmitter with $\pm 60^\circ$ beam scanning and 34.5 dBW EIRP," in *Proc. IEEE MTT-S Int. Microw. Symp.*, Boston, MA, USA, 2019, pp. 1064-1067.
- [3] J. R. Reis, M. Vala, and R. F. S. Caldeirinha, "Review paper on transmitarray antennas," *IEEE Access*, vol. 7, pp. 94171-94188, 2019.
- [4] J. G. Nicholls and S. V. Hum, "Full-space electronic beam-steering transmitarray with integrated leaky-wave feed," *IEEE Trans. Antennas Propag.*, vol. 64, no. 8, pp. 3410-3422, Aug. 2016.
- [5] C.-C. Cheng, B. Lakshminarayanan, and A. Abbaspour-Tamijani, "A programmable lens-array antenna with monolithically integrated MEMS switches," *IEEE Trans. Microwave Theory Tech.*, vol. 57, no. 8, pp. 1874-1884, Aug. 2009.
- [6] A. Clemente, L. Di Palma, F. Diaby, L. Dussopt, K. Pham, and R. Sauleau, "Electronically-steerable transmitarray antennas for Ka-band," in *Proc. 13th Eur. Conf. Antennas Propag. (EuCAP 2019)*, Krakov, Poland, 2019.
- [7] F. Foglia Manzillo, M. Smierzchalski, J. Reverdy, and A. Clemente, "A Ka-band beam-steering transmitarray achieving dual-circular polarization," in *Proc. 15th Eu. Conf. Antennas Propag. (EuCAP 2021)*, Dusseldorf, Germany, Mar. 2021.
- [8] P. Naseri, S. A. Matos, J. R. Costa, C. A. Fernandes, and N. J. G. Fonseca, "Dual-band dual-linear-to-circular polarization converter in transmission mode application to k/ka-band satellite communications," *IEEE Trans. Antennas Propag.*, vol. 66, no. 12, pp. 7128-7137, Dec. 2018.
- [9] K. T. Pham, R. Sauleau, E. Fourn, F. Diaby, A. Clemente, and L. Dussopt, "Dual-Band transmitarrays with dual-linear polarization at Ka-band," *IEEE Trans. Antennas Propag.*, vol. 65, no. 12, pp. 7009-7018, Dec. 2017.
- [10] A. Aziz, F. Yang, S. Xu, and M. Li, "An efficient dual-band orthogonally polarized transmitarray design using three-dipole elements," *IEEE Antennas Wireless Propag. Lett.*, vol. 17, no. 2, pp. 319-322, Feb. 2018.
- [11] Y. M. Cai, K. Li, W. Li, S. Gao, Y. Yin, L. Zhao, and W. Hu, "Dual-band circularly polarized transmitarray with single linearly polarized feed," *IEEE Trans. Antennas Propag.*, vol. 68, no. 6, pp. 5015-5020, Jun. 2021.
- [12] Z. Zhang, X. Li, C. Sun, Y. Liu, and G. Han, "Dual-band focused transmitarray antenna for microwave measurements," *IEEE Access*, vol. 8, pp. 100337-100345, 2020.
- [13] H. Hasani, J. S. Silva, S. Capdevila, M. Garcia-Vigueras, and J. R. Mosig, "Dual-band circularly polarized transmitarray antenna for satellite communications at 20/30 GHz," *IEEE Trans. Antennas Propag.*, vol. 67, no. 8, pp. 5325-5333, Aug. 2019.
- [14] M. Cai, Z. Yan, F. Fan, S. Yang, & X. Li, "Double-layer Ku/K dual-band orthogonally polarized high-efficiency transmitarray antenna". *IEEE Access*, 9, 89143-89149.
- [15] R. Madi., A. Clemente., and R. Sauleau, "Dual-band dual-linearly polarized transmitarray at Ka-band," in *Proc. 50th European Microwave Conference (EuMC)*, pp. 340-343, 2020.